Designing Ionic Liquids: Imidazolium Melts with Inert Carborane Anions

Anna S. Larsen, John D. Holbrey,† Fook S. Tham, and Christopher A. Reed*

Contribution from the Department of Chemistry, University of California, Riverside, California 92521-0403

Received March 1, 2000

Abstract: A new class of low-melting *N*,*N*′-dialkylimidazolium salts has been prepared with carborane counterions, some of the most inert and least nucleophilic anions presently known. The cations and anions have been systematically varied with combinations of 1-ethyl-3-methyl- ($EMIM^+$), 1-octyl-3-methyl- ($OMIM^+$), 1-ethyl-2,3-dimethyl- ($EDMIM^+$), and 1-butyl-2,3-dimethyl- ($BDMIM^+$) imidazolium cations and $CB_{11}H_{12}^-$, $CB_{11}H_6Cl_6^-$, and $CB_{11}H_6Br_6^-$ carborane anions to elucidate the factors which affect their melting points. From trends in melting points, which range from 156 °C down to 45 °C, it is clear that the alkylation pattern on the imidazolium cation is the main determinant of melting point and that packing inefficiency of the cation is the intrinsic cause of low melting points. C-Alkylation of the anion can also contribute to low melting points by the introduction of a further packing inefficiency. Nine of the thirteen salts have been the subject of X-ray crystal structural determination. Notably, crystallographic disorder of the cation is observed in all but one of these salts. It is the most direct evidence to date that packing inefficiency is the major reason unsymmetrical *N*,*N*′-dialkylimidazolium salts can be liquids at room temperature.

Introduction

Ionic liquids ("melts") are receiving renewed attention for their promise as alternative reaction media.[1−5] The important discovery was that *N*,*N*′-dialkylimidazolium[6,7] (**A**) and *N*-alkylpyridinium[8,9] (**B**) salts of common weakly coordinating anions (Y = $AlCl_4^-$, BF_4^-, $CF_3SO_3^-$, etc.) are liquids at or near room temperature. Other useful properties are negligible vapor

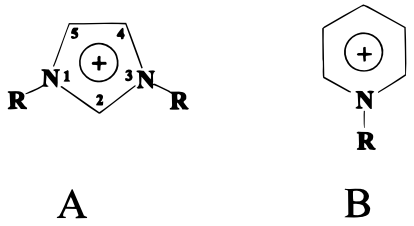

A B

pressure, high electrical conductivity, wide electrochemical window, tolerance to strong acids, and excellent thermal and chemical stability. The usable temperature ranges and unusual solvation characteristics of these media have added an important new dimension to traditional (i.e. metal halide) molten salt chemistry.[10−12]

Exactly *why* these salts have such low melting points is not well understood, although the asymmetry of the cation is believed to play a major role.

We have begun an investigation into the properties of a new class of imidazolium salts with two goals in mind. One is to shed light on the factors that contribute to the low melting points of *N*,*N*′-dialkylimidazolium salts. The other is to incorporate carborane anions into the ionic liquid repertoire. Carborane anions are among the most inert anions in modern chemistry. Their extraordinarily weak nucleophilicity and redox inertness has allowed the exploration of new extremes of cation reactivity[13] and the isolation of new superacids.[14,15] Their incorporation into ionic liquids should expand this utility, opening up new frontiers in reactive cation chemistry.

Despite their great stability, carborane anions are readily functionalized. For example, the 1-position (carbon) of the icosahedral $CB_{11}H_{12}^-$ ion can be alkylated and the 7−12 B−H bonds can be substituted with strong electrophiles (e.g. halogens). This allows a systematic variation of the properties of the anion that is unavailable in most traditional anions. Carboranes are 3D σ-aromatic analogues of arenes (2D π-aromatic systems) and the potential diversity of stable derivatives is comparable to that of substituted benzenes.[13]

* Address correspondence to this author. E-mail: chris.reed@ucr.edu.
† Current address: QUILL Centre, The Queen's University of Belfast, Stranmillis Rd., Belfast BT9 5AG, U.K. E-mail: j.holbrey@qub.ac.uk.

(1) Bradley, D. *Chem. Ind.* **1999**, *February 1*, 86.
(2) Freemantle, M. *C&E News* **1998**, *March 30*, 32−38. Freemantle, M. *C&E News* **2000**, *May 15*, 37−50.
(3) Chauvin, Y.; Olivier-Bourbigou, H. *Chemtech* **1995**, *September*, 26−30.
(4) Welton, T. *Chem. Rev.* **1999**, *99*, 2071−2083.
(5) Holbrey, J. D.; Seddon, K. R. *Clean Prod. Proc.* **1999**, *1*, 223−236.
(6) Wilkes, J. S.; Levisky, J. A.; Wilson, R. A.; Hussey, C. L. *Inorg. Chem.* **1982**, *21*, 1263−1264.
(7) Wilkes, J. S.; Zaworotko, M. J. *J. Chem. Soc., Chem. Commun.* **1992**, 965−967.
(8) Hurley, F. H.; Wier, T. P. *J. Electrochem. Soc.* **1951**, *98*, 203−206.
(9) Chum, H. L.; Koch, V. R.; Miller, L. L.; Osteryoung, R. A. *J. Am. Chem. Soc.* **1975**, *97*, 3264.
(10) Hussey, C. L. *Adv. Molten Salt Chem.* **1983**, *5*, 185−230.
(11) Hussey, C. L. *Pure Appl. Chem.* **1988**, *60*, 1763−1772.
(12) Seddon, K. R. *Molten Salt Forum* **1998**, *5*−*6*, 53−62.
(13) Reed, C. A. *Acc. Chem. Res.* **1998**, *31*, 133−139.
(14) Reed, C. A.; Fackler, N. L. P.; Kim, K.-C.; Stasko, D.; Evans, D. R.; Boyd, P. D. W.; Rickard, C. E. F. *J. Am. Chem. Soc.* **1999**, *121*, 6314−6315.
(15) Reed, C. A.; Kim, K.-C.; Bolskar, R. D.; Mueller, L. J. *Science* **2000**, *289*, 101−104.

10.1021/ja0007511 CCC: $19.00
Published on Web 07/18/2000

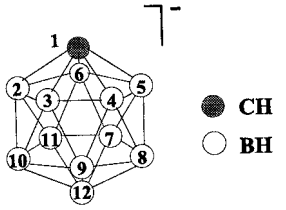

N,*N*′-Dialkylimidazolium cations are also readily functionalized in a systematic manner. Thus, imidazolium/carborane combinations can in principle lead to a very large number of salts with gradually varying properties. From trends in their melting points and spectroscopic data, and knowledge of their crystal structures, we can hope to identify the specific features of the cations and the anions that contribute to their lattice energies. Early studies on imidazolium-based ionic liquids led to 1-ethyl-3-methyl- and 1-butyl-3-methylimidazolium dialkylation patterns becoming favored in the popular $EMIM^+$ and $BMIM^+$ tetrachloroaluminate and tetrafluoroborate salts. The absence of strong H-bonding is certainly a major contributor to low melting points[7,16] but the role of weaker C(2)−H···Y (Y = anion) H-bonding-type interactions in these salts is open to debate.[17−19] Asymmetry of the cation is generally recognized to be an important factor. Recent systematic studies on 1-(n-C_nH_{2n+1})-3-methylimidazolium tetrafluoroborates for $n = 0-18$ reveal interesting trends in their melting (or glass) transition temperatures.[17] The $n = 1$ compound (i.e. 1,3-dimethylimidazolium) has a *higher* melting point than the N−H containing $n = 0$ compound, suggesting that the H-bonding influences are less than straightforward. The $n = 2-18$ compounds fall into two distinct groups. From $n = 2$ to 9, the compounds show glass transition temperatures rather than melting points, decreasing rapidly for $n = 2-4$ (i.e. ethyl through butyl) but remaining nearly constant (at ca. −80 °C) for $n = 4-9$. Curiously, the $n = 10-18$ compounds regain true melting points, at much higher temperatures (−4 through 60 °C), gradually increasing with increasing chain length.

Other factors that have been identified with respect to lowering melting points are burying or delocalization of the cation charge, the addition of solvent-like tails, nonalignment of ion pairs (cation stacking), buried charge in the anion (decreasing ionic bonding forces), and the minimalization of van der Waals forces.[7,20−25]

In the present study, we have concentrated our efforts on preparing imidazolium carborane salts with melting points just above room temperature. This offers a number of practical advantages without seriously jeopardizing their ultimate application as useful liquid reaction media. Synthesis, purification via recrystallization, and single crystal formation are all made easier by working with compounds that are solids at room temperature.

Experimental Section

All synthetic procedures were carried out in a Vacuum Atmospheres inert atmosphere (He) glovebox (O_2, H_2O < 1 ppm). Solvents were dried by passage through alumina columns (Anhydrous Engin.) which fed directly into the glovebox. IR spectra were recorded as KBr pellets on a Shimadzu FTIR-8300 spectrometer inside a nitrogen-atmosphere glovebox. ^{1}H NMR spectra in acetone-d_6 solutions were recorded on a 500 Inova Varian spectrometer. Microanalyses were performed by Desert Analytics Laboratories. Melting points were determined by differential scanning calorimetry (DSC) at 5 °C/min heating/cooling rate on 5−10 mg samples on a Shimadzu DSC-50 instrument equipped with dinitrogen cryostatic cooling. Quoted values were taken from the first peak of the second heating cycle, i.e., all samples were first melted and re-solidified before taking data. Some samples showed more than one peak on the heating trace, indicative of liquid crystal phase formation. Re-solidification temperatures upon cooling were frequently different from the melting point upon heating. They are given in the Experimental Section whereas melting points are listed later in a table.

Silver and cesium carborane salts[26,27] and imidazolium halides[17] were synthesized as described elsewhere. A representative procedure for the synthesis of an imidazolium carborane salt is described for **1**. Isolated yields were about 90% or better in all cases. Elemental analyses are given in Table S47 and NMR spectroscopic data are presented in Table 1. Traces (up to 0.25 equiv) of residual dichloromethane solvent were sometimes detectable in samples by NMR analysis.

[EMIM][$CB_{11}H_{12}$], 1. [EMIM]Cl (0.126 g, 0.856 mmol) was dissolved in dichloromethane (3 mL) and added to the stirred solution of Ag($CB_{11}H_{12}$) (0.215 g, 0.856 mmol) in methanol (30 mL). The solution immediately became cloudy. After 10 h of stirring, the precipitate was removed by filtration and the solvent was removed from the filtrate under reduced pressure. The resulting white waxy solid was redissolved in dichloromethane, filtered through Celite to separate the last traces of AgCl, and re-isolated by removal of the solvent under reduced pressure. The white crystals were dried under vacuum for 12 h (0.195 g, 90% yield). Crystals suitable for X-ray crystallography were grown by slow evaporation of a methanol solution at ambient temperature. In DSC, after melting at 122 °C, the material crystallized at 119 °C during the cooling cycle.

[EMIM][$CB_{11}H_6Cl_6$], 2. Synthesis was carried out according to the procedure described for **1** above from Cs[$CB_{11}H_6Cl_6$] and [EMIM]Cl in dichloromethane/acetone mixture (10:1 by volume). Crystals suitable for X-ray crystallography were grown by slow diffusion from dichloromethane solution layered with hexane at −30 °C. In DSC, after melting at 114 °C, the material crystallized at 109 °C during the cooling cycle.

[EMIM][$CB_{11}H_6Br_6$], 3. Synthesis was carried out according to the procedure described for **1** from Cs[$CB_{11}H_6Br_6$] and [EMIM]Cl in dichloromethane/acetone mixture (10:1 by volume). Crystals suitable for X-ray crystallography were grown in dichloromethane solution layered with hexane at ambient temperature. In DSC, after melting at 139 °C, the material crystallized at 99 °C during the cooling cycle.

[EMIM][1-Me-$CB_{11}H_{11}$], 4. Cs[1-Me-$CB_{11}H_{11}$] was obtained from treatment of [NMe_3H][$CB_{11}H_{12}$] with *n*-BuLi, followed by addition of CH_3I according to literature procedure,[27] and the product was recrystallized from isopropyl alcohol/water mixture saturated with cesium chloride. The synthesis of **4** was carried out according to the procedure described for **1** from Cs[1-Me-$CB_{11}H_{11}$] and [EMIM]Cl in dichloromethane. Additional purification was achieved via filtration of the reaction mixture through a small amount of alumina prior to the solvent removal. The product was recrystallized from methanol. In the DSC, after melting at 59 °C, the material did not crystallize during the cooling

(16) Suarez, P. A. Z.; Einloft, S.; Dullius, J. E. L.; de Souza, R. F.; Dupont, J. *J. Chim. Phys.-Chim. Biol.* **1998**, *95*, 1626−1639.
(17) Holbrey, J. D.; Seddon, K. R. *J. Chem. Soc., Dalton Trans.* **1999**, 2133−2139.
(18) Avent, A. G.; Chaloner, P. A.; Day, M. P.; Seddon, K. R.; Welton, T. *J. Chem. Soc., Dalton Trans.* **1994**, 3405−3413.
(19) Hitchcock, P. B.; Seddon, K. R.; Welton, T. *J. Chem. Soc., Dalton Trans.* **1993**, 2639−2643.
(20) Bonhôte, P.; Dias, A.-P.; Papageorgiou, N.; Kalyanasundaram, K.; Grätzel, M. *Inorg. Chem.* **1996**, *35*, 1168−1178.
(21) Golding, J. J. *Chem. Commun.* **1998**, 1593−1594.
(22) Sun, J.; Forsyth, M.; MacFarlane, D. R. *J. Phys. Chem. B* **1998**, *102*, 8858−8864.
(23) Karodia, N.; Guise, S.; Newlands, C.; Andersen, J.-A. *Chem. Commun.* **1998**, 2341−2342.
(24) Dickinson, E.; Williams, M. E.; Hendrickson, S. M.; Masui, H.; Murray, R. W. *J. Am. Chem. Soc.* **1999**, *121*, 613−616.
(25) MacFarlane, D. R.; Meakin, P.; Sun, J.; Amini, N.; Forsyth, M. *J. Phys. Chem. B* **1999**, *103*, 4164−4170.
(26) Plesek, J.; Jelinek, T.; Drdakova, E.; Hermanek, S.; Stibr, B. *Collect. Czech. Chem. Commun.* **1984**, *49*, 1559−1562.
(27) Jelinek, T.; Baldwin, P.; Scheidt, R. W.; Reed, C. A. *Inorg. Chem.* **1993**, *32*, 1982−1990.

Table 1. ^{1}H NMR Chemical Data (δ ppm, J Hz) in Acetone-d_6

		C^2H	C^4H	C^5H	NCH_2	NCH_3	$N(CH_2)_nCH_3$	C^2CH_3	$NCH_2(CH_2)_m$	$NC_2H_4CH_2$
1	EMIM $CB_{11}H_{12}$	9.32 (s)	7.81 (m)	7.74 (m)	4.43 (q, $J = 7.3$)	4.09 (s)	1.58 (t, $J = 7.3$)			
2	EMIM $CB_{11}H_6Cl_6$	9.09 (s)	7.81 (m)	7.74 (m)	4.44 (q, $J = 7.3$)	4.09 (s)	1.59 (t, $J = 7.3$)			
3	EMIM $CB_{11}H_6Br_6$	9.56 (s)	7.81 (m)	7.74 (m)	4.44 (q, $J = 7.3$)	4.09 (s)	1.59 (t, $J = 7.3$)			
4	EMIM 1-CH_3-$CB_{11}H_{11}$	9.29 (s)	7.82 (m)	7.75 (m)	4.44 (q, $J = 7.3$)	4.10 (s)	1.58 (t, $J = 7.3$)			
5	EMIM 1-C_2H_5-$CB_{11}H_{11}$	9.20 (s)	7.80 (m)	7.73 (m)	4.44 (q, $J = 7.3$)	4.09 (s)	1.58 (t, $J = 7.3$)			
6	EMIM 1-C_3H_7-$CB_{11}H_{11}$	9.10 (s)	7.81 (m)	7.74 (m)	4.44 (q, $J = 7.3$)	4.09 (s)	1.59 (t, $J = 7.3$)			
7	EMIM 1-C_4H_9-$CB_{11}H_{11}$	9.09 (s)	7.82 (m)	7.75 (m)	4.44 (q, $J = 7.3$)	4.09 (s)	1.58 (t, $J = 7.3$)			
8	OMIM $CB_{11}H_{12}$	9.10 (s)	7.81 (m)	7.75 (m)	4.39 (q, $J = 7.3$)	3.09 (s)	0.86 (t, $J = 7.3$)		1.45−1.20 (m = 6,12H)	
9	OMIM $CB_{11}H_6Cl_6$	9.11 (s)	7.81 (m)	7.75 (m)	4.40 (m)	4.10 (s)	0.86 (t, $J = 7.3$)		1.45−1.20 (m = 6,12H)	
10	EDMIM $CB_{11}H_{12}$		7.67 (m)	7.63 (m)	4.35 (q, $J = 7.3$)	3.98 (s)	1.50 (t, $J = 7.3$)	2.82 (s)		
11	EDMIM $CB_{11}H_6Cl_6$		7.67 (m)	7.63 (m)	4.35 (q, $J = 7.3$)	3.98 (s)	1.50 (t, $J = 7.3$)	2.81 (s)		
12	BDMIM $CB_{11}H_{12}$		7.66 (m)	7.63 (m)	4.31 (q, $J = 7.3$)	3.98 (s)	0.95 (t, $J = 7.3$)	2.82 (s)	1.87 (m = 1, 2H, m)	1.40 (2H, m)
13	BDMIM $CB_{11}H_6Cl_6$		7.67 (m)	7.63 (m)	4.32 (q, $J = 7.3$)	3.98 (s)	0.95 (t, $J = 7.3$)	2.82 (s)	1.87 (m = 1, 2H, m)	1.40 (2H, m)

cycle as the temperature was lowered to 25 °C. Crystallization did, however, occur slowly over a period of several days at ambient temperature.

[EMIM][1-Et-$CB_{11}H_{11}$], 5. Cs[1-Et-$CB_{11}H_{11}$] was obtained by treatment of [NMe_3H][$CB_{11}H_{12}$] with *n*-BuLi followed by addition of CH_3CH_2Br according to the literature procedure[27] and recrystallized from isopropyl alcohol/water mixture saturated with cesium chloride. The synthesis of **5** was carried out according to the procedure described for **1** from Cs[1-Et-$CB_{11}H_{11}$] and [EMIM]Cl in dichloromethane. Crystals of **5** suitable for X-ray crystallography were grown by slow diffusion in dichloromethane solution layered with hexane at −30 °C. In DSC, after melting at 64 °C, no crystallization was observed as the temperature was lowered to 25 °C. However, crystallization occurred slowly over a period of several days at ambient temperature.

[EMIM][1-Pr-$CB_{11}H_{11}$], 6. Cs[1-*n*-Pr-$CB_{11}H_{11}$] was obtained via treatment of [NMe_3H][$CB_{11}H_{12}$] with *n*-BuLi, followed by addition of *n*-C_3H_7Br according to literature procedure[27] and recrystallized from an isopropyl alcohol/water mixture saturated with cesium chloride. The synthesis of **6** was carried out according to the procedure described for **1** from Cs[1-Pr-$CB_{11}H_{11}$] and [EMIM]Cl in dichloromethane and recrystallized from ethanol solution layered with hexane at −10 °C. In DSC, after melting at 45 °C, no crystallization was observed as the temperature was lowered to 25 °C but crystallization did occur slowly after several days at ambient temperature.

[EMIM][1-Bu-$CB_{11}H_{11}$], 7. Cs[1-*n*-Bu-$CB_{11}H_{11}$] was obtained via treatment of [NMe_3H][$CB_{11}H_{11}$] with *n*-BuLi, followed by addition of *n*-C_4H_9Br according to literature procedure,[27] and recrystallized from isopropyl alcohol/water mixture saturated with cesium chloride. The synthesis of **7** was carried out according to the procedure described for **1** from Cs[1-Bu-$CB_{11}H_{11}$] and [EMIM]Cl in dichloromethane and recrystallized from dichloromethane solution layered with hexane at −30 °C. In DSC, after melting at 49 °C, no crystallization was observed as the temperature was lowered to 25 °C but crystallization did occur slowly after several days at ambient temperature.

[OMIM][$CB_{11}H_{12}$], 8. Synthesis was carried out according to the procedure described for **1** from Cs[$CB_{11}H_{12}$] and [OMIM]Cl in acetone/dichloromethane mixture (5:1 by volume). Crystals suitable for X-ray crystallography were grown by slow diffusion in dichloromethane solution layered with hexane at −30 °C. In DSC, after melting at 70 °C, no crystallization was observed as the temperature was lowered to 25 °C but crystallization did occur over a period of 24 h at ambient temperature.

[OMIM][$CB_{11}H_6Cl_6$], 9. Synthesis was carried out according to the procedure described for **1** above from Cs[$CB_{11}H_6Cl_6$] and [OMIM]Cl in dichloromethane. Crystals suitable for X-ray crystallography were grown by slow diffusion in dichloromethane solution layered with hexane at −30 °C. In DSC, after melting at 67 °C, no crystallization was observed as the temperature was lowered to 25 °C but crystallization did occur over a period of 24 h at ambient temperature.

[EDMIM][$CB_{11}H_{12}$], 10. Synthesis was carried out according to the procedure described for **1** from Cs[$CB_{11}H_{12}$] and [EDMIM]Br in dichloromethane/acetone mixture (5:1 by volume). Crystals suitable for X-ray crystallography were grown by slow diffusion in dichloromethane solution layered with hexane at −30 °C. In DSC, after melting at 156 °C, the material solidified at 155 °C during the cooling cycle.

[EDMIM][$CB_{11}H_6Cl_6$], 11. Synthesis was carried out according to the procedure described for **1** above from Cs[$CB_{11}H_6Cl_6$] and [EDMIM]-Br in dichloromethane. Crystals suitable for X-ray crystallography were grown by slow diffusion in dichloromethane solution layered with hexane at −30 °C. In DSC, after melting at 137 °C, the material solidified at 126 °C during the cooling cycle.

[BDMIM][$CB_{11}H_{12}$], 12. Synthesis was carried out according to the procedure described for **1** from Cs[$CB_{11}H_{12}$] and [BDMIM]Cl in acetone. The product was recrystallized from dichloromethane solution layered with hexane at −30 °C. In DSC, after melting at 129 °C, the material solidified at 117 °C during the cooling cycle.

[BDMIM][$CB_{11}H_6Cl_6$], 13. Synthesis was carried out according to the procedure described for **1** above from Cs[$CB_{11}H_6Cl_6$] and [BDMIM]-Cl in dichloromethane. Crystals suitable for X-ray crystallography were grown by slow diffusion in dichloromethane solution layered with hexane at −30 °C. In DSC, after melting at 101 °C, the material did not crystallize as the temperature was lowered to 25 °C but crystallization did occur slowly over a period of several days at ambient temperature.

X-ray Structure Determinations. Each sample crystal of compounds **1**−**5**, **9**−**11**, and **13** was mounted onto a glass fiber with epoxy resin. The X-ray intensity data were collected at low temperatures on a Bruker SMART 1000 CCD-based X-ray diffractometer system[28] with a Mo-target X-ray tube (λ = 0.71073 Å) operated at 2000 W power. A hemisphere of reflections (with a scan width of 0.3° in ω and with ϕ angles of 0°, 90°, 180°, and 0° for every 606, 435, 230, and 50 frames) was collected for all nine compounds. The experimental parameters

(28) SMART Software Reference Manual, version 5.054; Bruker Analytical X-ray Systems, Inc.: Madison, WI, 1997−1998.

Table 2. The Final Unit Cell Parameters and Structural Data Compounds **1**−**5**, **9**−**11**, and **13**

	1	**2**	**3**	**4**	**5**	**9**	**10**	**11**	**13**
crystal system	mono.	mono.	ortho.	mono.	mono.	ortho	mono.	mono.	ortho.
space group	$P2_1/c$	$P2_1/c$	$P2_12_12_1$	$P2_1/c$	$P2_1/c$	$P2_12_12_1$	$P2_1/c$	$P2_1/c$	$Pbca$
a (Å)	8.0681(19)	9.0438(7)	7.9007(4)	7.6953(5)	8.3037(13)	10.3552(5)	7.983(2)	13.2055(7)	18.5691(10)
b (Å)	21.136(2)	18.4443(14)	9.6217(5)	16.8607(11)	11.0683(13)	13.8856(6)	23.930(6)	11.1780(6)	14.9795(7)
c (Å)	9.9637(18)	12.8834(9)	29.5539(14)	13.5377(9)	19.760(2)	18.7681(9)	8.996(2)	15.3134(9)	35.1410(17)
α (deg)	90	90	90	90	90	90	90	90	90
β (deg)	111.32(2)	95.551(2)	90	101.761(2)	100.533(8)	90	104.847(5)	104.058(1)	90
γ (deg)	90	90	90	90	90	90	90	90	90
V (Å^3)	1582.8(5)	2139.0(3)	2246.63(19)	1719.6(2)	1785.5(4)	2698.6(2)	1661.2(7)	2192.7(2)	9774.7(8)
Z	4	4	4	4	4	4	4	4	16
Fw	254.18	460.85	727.56	268.21	282.24	544.99	268.21	474.88	502.93
D_c (g/cm^3)	1.067	1.431	2.151	1.036	1.050	1.341	1.072	1.439	1.367
temp (K)	198(2)	228(2)	208(2)	273(2)	198(2)	198(2)	198(2)	198(2)	198(2)
GOF on F^2	1.079	1.032	1.037	1.039	1.065	1.052	1.048	1.084	1.045
$R1$ ($I > 2\sigma I$)	0.0529	0.0466	0.0387	0.0509	0.0466	0.0327	0.0541	0.0326	0.0461
$R1$ (all)	0.0815	0.0697	0.0621	0.0703	0.0650	0.0390	0.0810	0.0424	0.0784
$wR2$ ($I > 2\sigma I$)	0.1348	0.1193	0.0711	0.1447	0.1350	0.0826	0.1434	0.0837	0.1035
$wR2$ (all)	0.1487	0.1305	0.0744	0.1606	0.1466	0.0856	0.1561	0.0882	0.1140
diff. pk/ho (e/Å^3)	0.20/−0.82	1.31/−0.29	1.02/−0.82	0.11/−0.19	0.23/−0.20	0.41/−0.40	0.20/−0.23	0.46/−0.40	1.22/−0.23

used for data acquisition are summarized in Table S46 of the Supporting Information. The frames were integrated with the Bruker SAINTPLUS software package[29] using a narrow-frame integration algorithm. The data frames from compounds **1**, **2**, **4**, **5**, **10**, and **11** were integrated as a monoclinic crystal system and those from compounds **3**, **9**, and **13** were integrated as an orthorhombic crystal system. The Bruker SHELXTL (Version 5.1)[30] software package was used for data reduction and the results are summarized in Table S46. The Bruker SHELXTL (Version 5.1)[30] software package was used for phase determination and structure refinement for all nine compounds. The FLAT (for compounds **2** and **11**), DFIX (for compounds **9** and **13**), DELU (for compound **13**), SIMU (for compounds **4** and **13**), and SAME (for compounds **1**, **2**, **4**, **5**, **9**, **10**, **11**, and **13**) restraints were used during structure refinement. The results are tabulated in Table 2.

[EMIM][$CB_{11}H_{12}$], 1: $C_7H_{23}B_{11}N_2$. No absorption correction was applied to the raw intensity data. The distribution of intensities and systematic absent reflections ($E^2 - 1 = 0.982$, centrosymmetric) indicated one possible space group, $P2_1/c$. Direct methods of phase determination followed by two Fourier cycles led to an electron density map from which most of the non-hydrogen atoms were identified. Subsequent isotropic refinement led to the identification of the remaining non-hydrogen atoms, including the disordered cation atoms. The imidazolium cation was modeled as a disorder having approximate 2-fold rotation symmetry, with the symmetry axis almost parallel to the direction of the C2−C5 carbon. The site occupation ratio was 74/26%. Atomic coordinates and isotropic and anisotropic temperature factors of all the non-hydrogen atoms were refined by means of a full-matrix least-squares procedure on F^2. All of the H-atoms were included in the refinement in calculated positions riding on the atoms to which they were attached.

[EMIM][$CB_{11}H_6Cl_6$], 2: $C_7H_{17}B_{11}Cl_6N_2$. Data collection and refinement were carried out as with **1**. The imidazolium cation was modeled as a disorder having approximate mirror plane symmetry in the plane of the imidazolium ring but rotated about 20°. The site occupation ratio was 70/30%.

[EMIM][$CB_{11}H_6Br_6$], 3: $C_7H_{17}B_{11}Br_6N_2$. The SADABS[30] absorption correction was applied to the raw intensity data ($\mu = 10.719$ mm^{-1}, max/min transmission = 0.8020/0.4243). The distribution of intensities and systematic absent reflections ($E^2 - 1 = 0.751$, noncentrosymmetric) indicated one possible space group, $P2_12_12_1$. Direct methods of phase determination followed by two Fourier cycles led to an electron density map from which all of the non-hydrogen atoms were identified. No disorder was observed in the imidazolium cation or the carborane anion.

[EMIM][1-Me-$CB_{11}H_{11}$], 4: $C_8H_{25}B_{11}N_2$. Data collection and refinement were carried out as with **1**. The imidazolium cation was modeled as a disorder having approximate mirror plane symmetry in the plane of the imidazolium ring but rotated about 10°. The anion was modeled as disordered with the pentagonal boron belts tilted about 53° from one another. The site occupation ratios for the disordered cations and disordered anions were 72/28% and 75/25%, respectively.

[EMIM][1-Et-$CB_{11}H_{11}$], 5: $C_9H_{27}B_{11}N_2$. No absorption correction was applied to the raw intensity data. The distribution of intensities and systematic absent reflections ($E^2 - 1 = 0.967$, centrosymmetric) indicated three possible space groups, $P2_1/c$, Pc, and $P2/c$. The combined figure of merit indicated $P2_1/c$ to be the most likely space group, which was later determined to be correct. Direct methods of phase determination followed by two Fourier cycles led to an electron density map from which most of the non-hydrogen atoms were identified. Subsequent isotropic refinement led to the identification of the rest of the non-hydrogen atoms, including the disordered cation atoms which were modeled as a slight displacement disorder. The site occupation ratio was 51/49%.

[OMIM][$CB_{11}H_6Cl_6$], 9: $C_{13}H_{29}B_{11}Cl_6N_2$. No absorption correction was applied to the raw intensity data. The distribution of intensities and systematic absent reflections ($E^2 - 1 = 0.831$, noncentrosymmetric) indicated one possible space group, $P2_12_12_1$. Direct methods of phase determination followed by two Fourier cycles led to an electron density map from which most of the non-hydrogen atoms were identified. Subsequent isotropic refinement led to the identification of the rest of the non-hydrogen atoms, including the disordered atoms of the octyl imidazolium cation which were modeled as a rotational disorder. The site occupation ratio was 71/29%. For anion−anion interactions, the closest C−H···Cl distances (Å) are 3.03, 2.97 and angles (deg) are 133, 131, respectively. For the major component of the disordered cation, the closest C−H···Cl distances (Å) are 3.06, 2.93, 3.01, 3.14, 2.86 and angles (deg) are 127, 128, 149, 120, 163, respectively. The shortest perpendicular distance from a Cl atom to the mean 5-atom plane of the aromatic ring is 3.33 Å.

[EDMIM][$CB_{11}H_{12}$], 10: $C_8H_{25}B_{11}N_2$. Data collection and refinement were carried out as with **1**. The disordered cations were modeled with approximate mirror plane symmetry, the mirror plane being almost perpendicular to the plane of the five-membered ring and along the direction of the N1−N3 vector. The site occupation ratio was 62/38%.

[EDMIM][$CB_{11}H_6Cl_6$], 11: $C_8H_{19}B_{11}Cl_6N_2$. Data collection and refinement were carried out as with **1**. The disordered cations were modeled with approximate mirror plane symmetry, hinged at the N3 position like the wings of a butterfly. The site occupation ratio was 86/14%. Considering only the major component of the disordered cations, the C−H···Cl distances (Å) are 2.90, 2.74 and angles (deg) are 173, 161, respectively. The shortest perpendicular distance between one of the six Cl atoms to the mean 5-atom plane of the aromatic ring is 3.13 Å.

[BDMIM][$CB_{11}H_6Cl_6$], 13: $C_{10}H_{23}B_{11}Cl_6N_2$. No absorption correction was applied to the raw intensity data. The distribution of intensities

(29) SAINTPLUS Software Reference Manual, version 5.02; Bruker Analytical X-ray Systems, Inc.: Madison, WI, 1997−1998.

(30) SHELXTL Software Reference Manual, version 5.1; Bruker Analytical X-ray Systems, Inc.: Madison, WI, 1997−1998.

Scheme 1

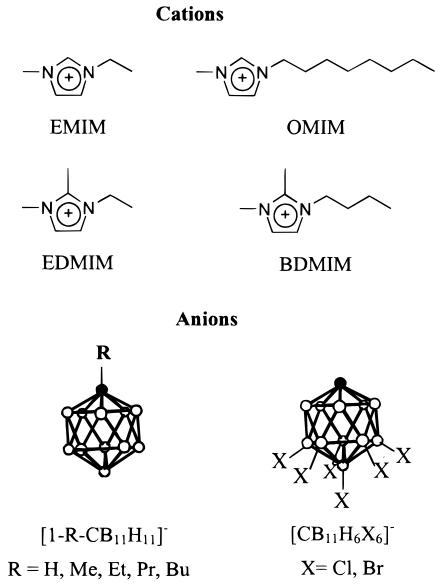

and systematic absent reflections ($E^2 - 1 = 0.897$, centrosymmetric) indicated one possible space group, *Pbca*. Direct methods of phase determination followed by two Fourier cycles led to an electron density map from which most of the non-hydrogen atoms were identified. Subsequent isotropic refinement led to the identification of the remaining non-hydrogen atoms, including the disordered cation atoms. There are two imidazolium cations and two carborane anions in the asymmetric unit. Only one of the two imidazolium cations was modeled as a disordered cation. The aromatic ring and the 2,3-methyl groups have a "sliding disorder" and the butyl side chain has rotational disorder. The site occupation ratio for the disordered cation was 78/22%. Considering the anion−anion contacts, the C−H···Cl distances (Å) are 2.96, 3.13, 3.10 and angles (deg) are 142, 141, 136, respectively. For the fully occupied cation, the cation−anion C−H···Cl distances (Å) are 3.14, 3.18, 2.80 and angles (deg) are 132, 141, 133, respectively. For the major component of the disordered cation, the cation−anion C−H···Cl distances (Å) are 2.94, 3.15 and angles (deg) are 163, 122, respectively. The shortest perpendicular distance between one of the six Cl atoms to the mean 5-atom plane of the fully occupied aromatic ring is 3.25 Å.

Results and Discussion

Synthesis. Scheme 1 shows the cations and anions used in this study. Imidazolium carborane salts were obtained by metathesis reactions of silver or cesium carboranes with imidazolium chlorides or bromides in varying solvents. The best routes typically involved cesium rather than silver salts in dichloromethane, frequently with a small amount of acetone added to increase solubility of the cesium reagent. Under these conditions, satisfactory separation of the cesium halide byproduct was usually achieved with a single filtration. Complete precipitation of silver halides from organic solvents can be quite slow, leading to silver-contaminated products. The imidazolium carborane salts **1**−**13** were isolated and characterized by ^{1}H NMR spectroscopy, elemental analysis, DSC, and single crystal X-ray diffraction methods. In pure form, they are white crystalline solids at ambient temperature. Most of the salts are only mildly hygroscopic, can be safely stored in a desiccator, and can be handled briefly in air. All have high solubility in dichloromethane, common alcohols, and acetone but low solubility in water.

The melting points for compounds **1**−**13**, determined from the first peak in their DSC traces, are presented in Table 3. In general, carborane salts with other types of cations melt (or decompose without melting) above ca. 300 °C. For example, $[Me_4N][12\text{-Et-}CB_{11}H_{11}]$ melts with decomposition at 330 °C.[31] Thus, it is the introduction of an unsymmetrically dialkylated imidazolium cation that dramatically lowers melting points. In the carborane salts **1**−**13,** the melting temperatures lie in the range 45−156 °C. Many of the melted compounds exhibit a tendency to supercool, remaining in a glassy state for prolonged periods of time before recrystallizing.

Table 3. Melting Points and Density Data

	compd	mp, °C	densit,y g/cm^3
1	$[EMIM][CB_{11}H_{12}]$	122	1.067
2	$[EMIM][CB_{11}H_6Cl_6]$	114	1.431
3	$[EMIM][CB_{11}H_6Br_6]$	139	2.151
4	$[EMIM][1\text{-}CH_3\text{-}CB_{11}H_{11}]$	59	1.036
5	$[EMIM][1\text{-}C_2H_5\text{-}CB_{11}H_{11}]$	64	1.050
6	$[EMIM][1\text{-}C_3H_7\text{-}CB_{11}H_{11}]$	45	
7	$[EMIM][1\text{-}C_4H_9\text{-}CB_{11}H_{11}]$	49	
8	$[OMIM][CB_{11}H_{12}]$	70	
9	$[OMIM][CB_{11}H_6Cl_6]$	67	1.341
10	$[EDMIM][CB_{11}H_{12}]$	156	1.072
11	$[EDMIM][CB_{11}H_6Cl_6]$	137	1.439
12	$[BDMIM][CB_{11}H_{12}]$	129	
13	$[BDMIM][CB_{11}H_6Cl_6]$	101	1.367

Trends in Melting Points. The first observation to be made from the data in Table 3 is that in salts where the carborane anion is not C-alkylated, i.e., compounds **1**−**3** and **8**−**13**, the nature of the imidazolium cation is clearly the main determinant of melting point. This is presented graphically in Figure 1. The melting point of the $CB_{11}H_6Cl_6^-$ salt for a particular cation closely tracks that of its $CB_{11}H_{12}^-$ salt, some 3 to 28 °C lower in temperature. Within this data set, the lowest melting points are achieved with the cation having the longest alkyl chain, i.e., octyl in the $OMIM^+$ salts **8** and **9**. This is also true within the subset of data for *tri*alkylated imidazolium cations. For a particular anion, the *butyl*dimethyl cation leads to a lower melting point than the *ethyl*dimethyl cation (compare **10** with **12** or **11** with **13**). The increasing disruption of crystal packing as the chain length is extended apparently overrides increased van der Waals interactions between the larger components.

Methylation of the C-2 position of the imidazolium cation does not lower melting points in the present compounds. In fact, 1-ethyl-2,3-*di*methyl salts **10** and **11** have melting points some 20−30° *higher* than their 1-ethyl-3-methyl counterparts **1** and **2**. This is a somewhat unexpected result in view of the acidity of the C(2)−H protons of an imidazolium ring and the possibility that they could engage in H-bonding to anions. Indeed, the chemical shifts of the C(2)−H protons show an anion dependence in acetone, suggestive of H-bonding in ion pairs in solution (see Table 1). They vary over a 0.5 ppm range whereas all the other imidazolium protons have constant chemical shifts within experimental error (0.02 ppm). With small anions such as chloride and nitrate, H-bonding of this kind has been established in imidazolium melts by NMR spectroscopy[32] and in solids by X-ray crystallography[33] but with BF_4^- the evidence is inconclusive.[17] With large carborane anions, imidazolium C(2)−H interactions are apparently significant only in the specific ion pairs that are assumed to form in solution. In the global, more isotropic electrostatic fields of the melted and solid

(31) Gruner, B.; Janousek, Z.; King, B. T.; Woodford, J. N.; Wang, C. H.; Vsetecka, V.; Michl, J. *J. Am. Chem. Soc.* **1999**, *121*, 3122−3126.

(32) Elaiwi, A.; Hitchcock, P. B.; Seddon, K. R.; Srinivasan, N.; Tan, Y.-M.; Welton, T.; Zora, J. A. *J. Chem. Soc., Dalton Trans.* **1995**, 3467−3471.

(33) Abdul-Sada, A. K.; Greenway, A. M.; Hitchcock, P. B.; Mohammed, T. J.; Seddon, K. R.; Zora, J. A. *J. Chem. Soc., Chem. Commun.* **1986**, 1753−1754.

Table 4. Dominant Infrared Bands Observed above 3000 cm^{-1}

	compd	νC(5)−H and νC(4)−H		νC(2)−H	νC−H (carborane)
1	[EMIM][$CB_{11}H_{12}$]	3168(s)	3151(s)	3125(s),	3048(w)
2	[EMIM][$CB_{11}H_6Cl_6$]	3166(s)	3151(s)	3128(m), 3115(m)	3067(s)
3	[EMIM][$CB_{11}H_6Br_6$]	3162(s)	3142(s)	3099(s)	3053(s)
4	[EMIM][1-CH_3-$CB_{11}H_{11}$]	3168(s)	3150(m)	3123(m)	
5	[EMIM][1-C_2H_5-$CB_{11}H_{11}$]	3164(s)	3144(s)	3117(m), 3106(m)	
6	[EMIM][1-C_3H_7-$CB_{11}H_{11}$]	3162(s)	3144(m)	3115(s)	
7	[EMIM][1-C_4H_9-$CB_{11}H_{11}$]	3164(s)	3149(m)	3118(s)	
8	[OMIM][$CB_{11}H_{12}$]	3165(s)	3148(m)	3122(m)	3061(m)
9	[OMIM][$CB_{11}H_6Cl_6$]	3176(m)	3152(vs)	3117(m), 3101(m)	3063 (s)
10	[EDMIM][$CB_{11}H_{12}$]	3183(m)	3148(s)		3046(w)
11	[EDMIM][$CB_{11}H_6Cl_6$]	3179(m)	3145(s)		3063(s)
12	[BDMIM][$CB_{11}H_{12}$]	3181(m)	3146(s)		3049(m)
13	[BDMIM][$CB_{11}H_6Cl_6$]	3179(m)	3145(s)		3075(s), 3058(s), 3047(w)

Table 5. Close Cl···Cation Distances (Å) and Angles (deg) for [EMIM][$CB_{11}H_6Cl_6$], **2**

atom nos.		distances		angles
H	Cl	H···Cl	Cl···C	C−H···Cl
4″A	2C	3.14	3.74	123
4″A	3C	2.83	3.67	148
4″A	6C	3.07	3.76	132
2″A	1	2.89	3.70	145
2″A	4B	3.16	3.85	132
5″A	4D	2.96	3.86	160

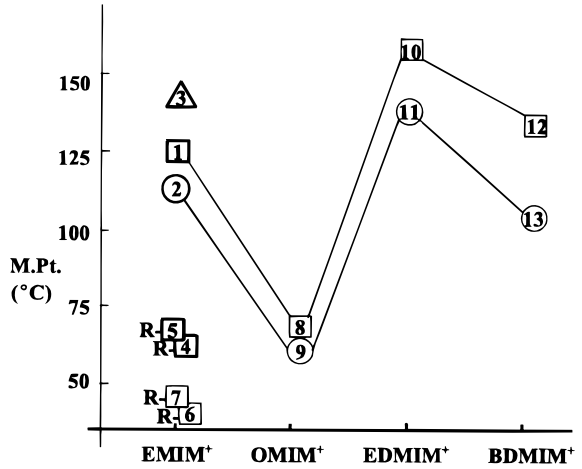

Figure 1. Melting points as a function of cation and anion: (□) for $CB_{11}H_{12}^-$ salts, (○) for $CB_{11}H_6Cl_6^-$ salts, and (△) for $CB_{11}H_6Br_6^-$ salts. C-Alkylated 1-R-$CB_{11}H_{11}^-$ salts are indicated as R-□.

states, they are apparently of less importance. Supporting evidence for this view comes from the X-ray structures and IR spectra discussed below. Placing a methyl group in the 2-position of an already *N*-methylated imidazolium cation may, in fact, aid packing efficiency by masking the 1,3-dialkylation asymmetry, thereby raising melting points.

The melting point data for compounds **1**−**7**, all with the same $EMIM^+$ cation, are informative with respect to the role of the anion. The compounds fall into two clearly discernible groups, those with C-alkylation of the carborane and those without. Comparing **1**, **2**, and **3,** it is apparent that 7−12 hexahalogenation of the $CB_{11}H_{12}^-$ carborane is not of particularly great consequence. This is a little surprising because the "boron end" of a carborane anion is more electron rich than the carbon end, and therefore most likely to make contact with the imidazolium cation in ion-pairing interactions. The polarity of the carborane anion is well established in studies with coordinating cations such as Ag^+ and R_3Si^+ where bonding always occurs via the 7−12 B−H or B−X substituents.[34] One might have expected that the substituent change from B−H to B−Cl (or B−Br) would have altered the cation/anion interactions in a more significant way because the overall dipole of the $CB_{11}H_{12}^-$ anion must be significantly increased by 7−12 hexahalogenation. The lack of a substantial effect on melting points suggests that the overall dipole of the anion is not a particularly important contributor to the lattice energy. The delocalized anionic charge of the carborane resides in the CB_{11} framework and its unsymmetrical distribution is to some degree camouflaged by the layer of hydrogen and/or halogen atom substituents. The charge and its polarity are apparently not sensed strongly by a noncoordinating cation such as the imidazolium ion in the relatively isotropic electrostatic field of the crystal and melted states. This suggests that when searching for significant cation/anion interactions in the crystal structures of the salts we should concentrate on local effects rather than alignment of dipoles. The melting points of **1**, **2**, and **3** suggest that the order of increasing local interaction of the anion substituents with the cation may be Cl < B−H < Br. The differences are slight, however. Perhaps the additivity of dispersion forces (higher for Cl and Br) and local polarities (higher for the hydridic B−H bonds) makes their interactions with cations roughly equivalent. An alternative way of understanding this is to consider the size of the anion. Although the halide substituents add electrons and therefore increase dispersion forces, they also lower the electrostatic contribution to the lattice energy by making the anion larger. These effects are roughly equivalent and the melting points are not particularly anion dependent.

Nevertheless, introduction of a C-alkyl substituent onto the carborane anion in compounds **4**, **5**, **6**, and **7** leads to a substantial drop (ca. 60 °C) in the melting temperatures of the $EMIM^+$ salts, relative to **1**, **2**, and **3**. C-Alkylation of the anion is not expected to alter its dipole in a very significant manner so, once again, the data suggest that the overall dipole of the anion is not a major determining factor. The C(1)−H bond of the carborane anion is somewhat acidic (it reacts with BuLi) but it cannot be expected to interact significantly with the positively charged imidazolium ion. Indeed, no particularly significant interactions can be discerned in the crystal structures and the carborane C−H stretching frequency varies by only 29 cm^{-1} in all of the unalkylated salts (see below). Thus, C-alkylation of the $CB_{11}H_{12}^-$ anion is not expected to break up any cation/anion interactions in **1**, **2**, and **3** that might rationalize a 60° drop in the melting points of **4**−**7**. We hypothesize therefore that C-alkylation of the carborane introduces a new appendage to the anion, diminishing its ability to pack efficiently.

(34) Xie, Z.; Manning, J.; Reed, R. W.; Mathur, R.; Boyd, P. D. W.; Benesi, A.; Reed, C. A. *J. Am. Chem. Soc.* **1996**, *118*, 2922−2928.

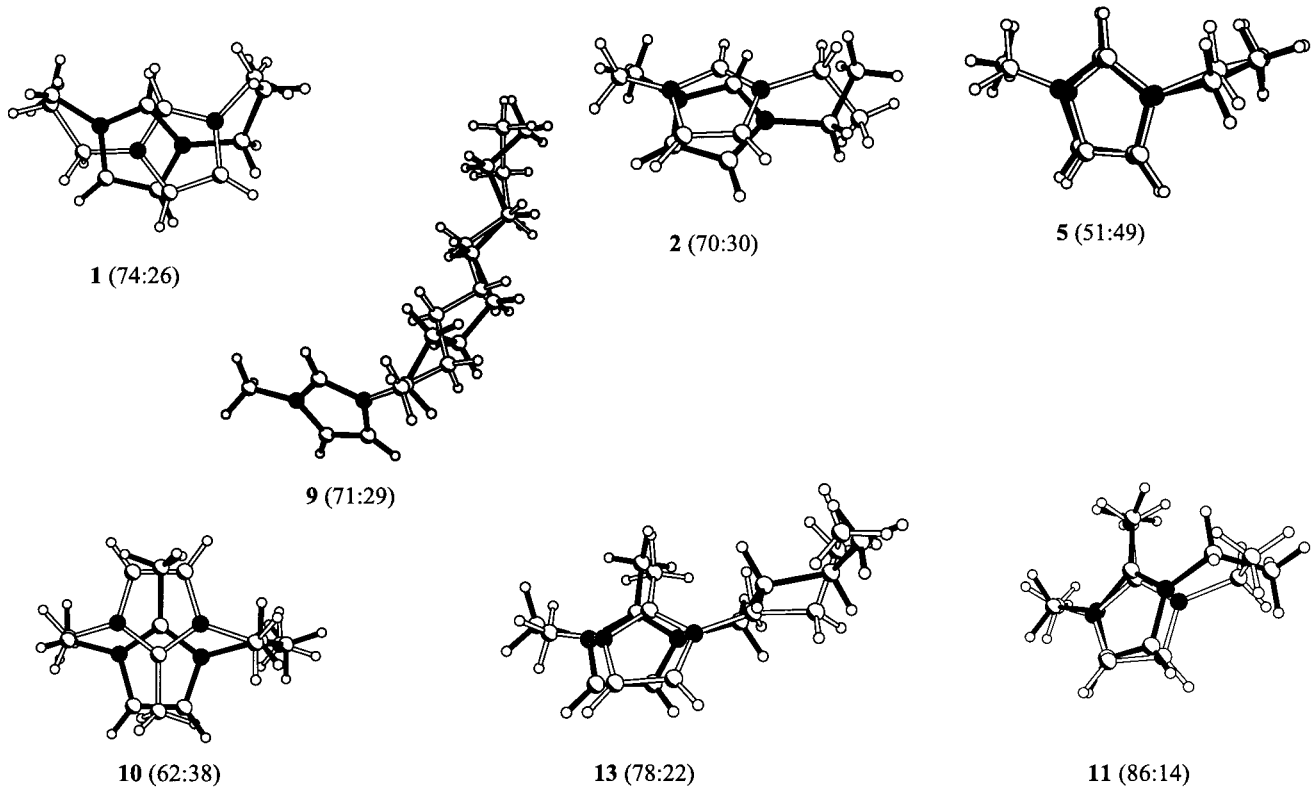

Figure 2. Examples of imidazolium cation disorder. The minor component (open bonds) is overlaid onto the major component (solid bonds) and the percentage ratio is indicated in parentheses after the compound number. Nitrogen atoms are indicated by solid circles.

Combining the trends in cation and anion effects on melting points leads to the prediction that octylmethylimidazolium salts of the type [OMIM][1-R-$CB_{11}H_{11}$] will be liquids at room temperature for R = Me, Et, *n*-Pr, and *n*-Bu. This seems to be the case but to date we have been unable to prepare entirely analytically pure samples of the viscous hygroscopic glasses that result from preparative metathesis reactions. In addition, 1-*ethyl*-3-methylimidazolium salts of 1-R-$CB_{11}H_{11}^-$ anions with longer R (C_5-C_{12} *n*-aliphatic) appear to be room temperature liquids but their investigation also awaits the development of clean preparative routes.

Infrared Spectra. There has been considerable debate in the imidazolium salt literature over the significance of small frequency shifts in the C−H stretching frequencies of the cations and whether they accurately reflect the degree of H-bonding to anions. Table 4 lists the dominant infrared bands for compounds **1**−**13** observed above 3000 cm^{-1}. This region is considered diagnostic of the two (or three) aromatic C−H bonds of the cations. It is also the region where the single stretching frequency of the C−H bond of the carborane anion appears. Not listed in the table are a number of weak or very weak bands and shoulders that can be variously assigned to overtones, solid-state splitting, or multiplicities arising from crystallographic disorder. Actual spectra are available as Supporting Information.

We assign the two highest frequencies to the C(4)−H and C(5)−H stretches. The highest frequency band appears at 3137−3133 cm^{-1} in [EMIM]X (X = Cl, Br, I)[32] and lies within the 3183−3162 cm^{-1} range in compounds **1**−**13**. The higher values in the present compounds suggest that the weak C−H···anion H-bonding-type interactions believed to be present in the halide salts are diminished or absent in the carborane salts. Within the 13 carborane salts, the small range (only 21 cm^{-1}) suggests that C−H interactions with the anions vary in only a trivial manner. Data for the second highest frequency band vary by only 10 cm^{-1}, reinforcing the notion that C(4)−H and C(5)−H interactions with the anions are very weak.

The third highest frequency is assigned to the stretching frequency of the C(2)−H bond of the imidazolium ion. Adjacent to both N atoms of the cation it is logically less electron-rich and thus more prone to H-bonding than the C(4)−H or C(5)−H bonds. The range of frequencies is 3125−3099 cm^{-1} and in a number of the compounds there are shoulders or splitting into two medium intensity bands. The somewhat greater range (26 cm^{-1}) suggests a slightly greater proclivity toward varied interactions with the anions and this tends to be borne out in the crystallographic observations made below. The frequent duality of bands may be a reflection of the cation disorder observed in the crystal structures. As expected, this band is absent in the 2-methylated imidazolium salts **10**−**13**.

The fourth highest frequency is assigned to the unique C−H stretch of the carborane and lies in the range 3075−3046 cm^{-1}. With the exception of the somewhat high 3075 cm^{-1} band (of three) in **13**, the range is about the same as we have observed in a large number of carborane salts and probably reflects nothing more than the normal range of van der Waals interactions that the carbon end of the anion experiences with other components of the crystal lattice. Sometimes a minor splitting is observed to lower energy but this again is the same as we have observed in a variety of other carborane salts. Its most logical explanation is solid-state splitting arising from crystal site asymmetry. As expected, this band is absent in the C-alkylated carborane salts **4**−**7**.

X-ray Structures. Crystal structures have been determined for 9 of the 13 imidazolium salts: compounds **1**−**5**, **9**−**11**, and **13**. Probably the most important observation is that in all but one of the structures, the imidazolium cation is disordered. As illustrated in Figure 2 by overlaying the major and minor occupancies, the disorder can take many different forms. For

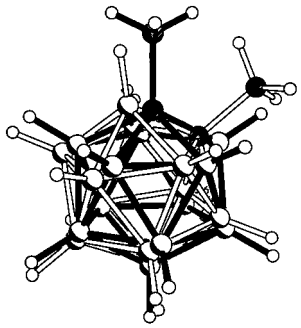

Figure 3. Disorder in the C-methylated carborane anion of [EMIM]-[1-Me-$CB_{11}H_{11}$], **4**.

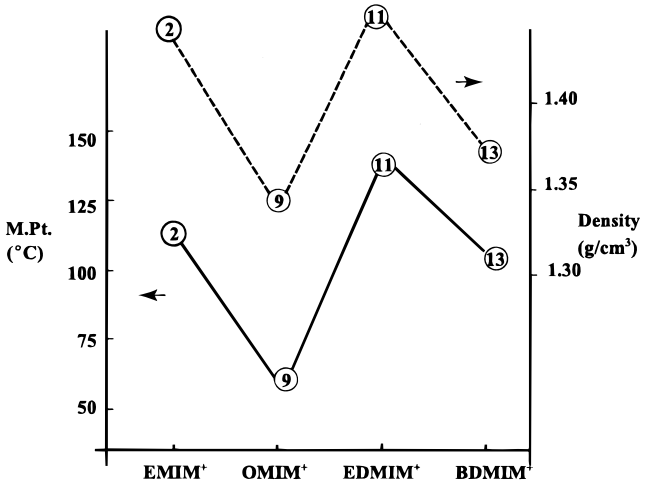

Figure 4. Correlation of calculated crystal densities of $CB_{11}H_6Cl_6^-$ salts (dashed line) with melting points (solid line) as a function of cation.

the cations with the shorter alkyl chains, the disorder always involves the imidazolium ring. For the cation with the longest alkyl group, octyl in **9**, the disorder is confined to the aliphatic chain. Inspection of the positions of the terminal methyl groups finds frequent near spatial coincidence in the major and minor forms. This shows that the disorder is accommodated within about the same cavity size.

The carborane anion is ordered in all but one structure. Interestingly, the disorder occurs with the C-methylated anion in **4**, one of the lowest melting compounds. The disorder is illustrated in Figure 3.

The only structure *without* disorder, in either the carborane or imidazolium fragments, is [EMIM][$CB_{11}H_6Br_6$], **3**. Notably, this compound also has the second *highest* melting point.

We interpret disorder in the cation as a direct reflection of the poor packing efficiency of the imidazolium ions. It is consistent with the notion that low symmetry is the single most important attribute of *N*,*N*′-dialkylimidazolium ions in conferring low melting points on their salts. Indeed, our analysis of the trends in melting points discussed above seemed to point toward this as the major cause of lowered melting points. The trends in melting points are also reflected in crystal densities (Table 3). Figure 4 shows how, for a particular anion ($CB_{11}H_6Cl_6^-$) for which there are data for all cations, the calculated crystal densities follow the same trend as the melting points in their dependency on the nature of the cation.

Of the eight crystal structures that have previously been determined for [EMIM]Y salts (Y = iodide,[33] chloride,[32,35] nitrate,[7] hexafluorophosphate,[36] tetracyano-*p*-quinodimethanide,[37]

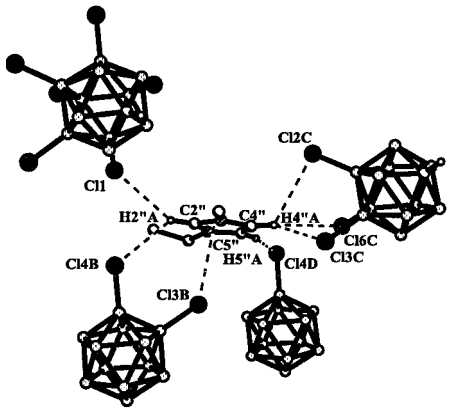

Figure 5. View of the close cation/anion interactions in the X-ray structure of **2**. Many of the carborane chlorine atoms not involved in interactions with the cation are omitted for clarity.

bromide,[32] tetrabromoaluminate,[32] and tetrachloropalladate[38]), only the chloride is reported to have disorder. However, we note that all of these salts have relatively small and/or charge-exposed anions and that in each of these crystal structures, H-bonding or stacking interactions have been identified in the lattice. These interactions apparently lead to the high degree of order that is observed. By contrast, the large, charge-diffuse carboranes used in the present work appear to have diminished specific cation/anion interactions to the point where packing inefficiencies are manifest in obvious and frequent disorder.

Inspection of the stereoscopic packing diagrams for the nine structures (see Supporting Information) does not reveal any obvious patterns in the packing of the carborane anions. Sometimes their mutual orientations are consistent with anion/anion dipole alignment, but most often they are not. In **1**, the closest approaching carboranes actually have their dipoles in a repulsive orientation. Similarly, the C_5 axis of the carborane shows no obvious pattern of electrostatic alignment with the closest approaching cation. These observations tend to confirm that the overall dipolar nature of the carborane anion is not a very important contributor to lattice energy.

For each of the structures we have inspected the closest cation/anion contacts in an attempt to identify the most significant local attractive interactions that may contribute to the lattice energy. In all of the structures containing the $CB_{11}H_6Cl_6^-$ anion, chlorine atoms make the closest approaches to a cation. For the purposes of defining the most significant C−H···Cl interactions we have limited ourselves to the consideration of H···Cl distances <3.20 Å and C−H···Cl angles >120°. These dimensions are based on the sum of the van der Waals radii for hydrogen and chlorine and the supposition that the energy of interaction will be highest for those C−H···Cl geometries that approach linearity.[36] The limits are arbitrary and are not meant to deny the continuum of weak C−H···Cl interactions that contribute to lattice energetics.[39] These limits easily encompass the majority of such interactions.[39] A representative example of these cation/anion interactions is shown in Figure 5 for compound **2**. All three aromatic protons of the

(35) Dymek, C. J., Jr.; Grossie, D. A.; Fratini, A. V.; Adams, W. W. *J. Mol. Struct.* **1989**, *213*, 25−34.
(36) Fuller, J.; Carlin, R. T.; De Long, H. C.; Haworth, D. *J. Chem. Soc., Chem. Commun.* **1994**, 299−300.
(37) Grossel, M. C.; Hitchcock, P. B.; Seddon, K. R.; Welton, T.; Weston, S. C. *Chem. Mater.* **1994**, *6*, 1106−1108.
(38) Ortwerth, M. F.; Wyzlic, M. J.; Baughman, R. G. *Acta Crystallogr.* **1998**, 1594−1596.
(39) Aakeroy, C. B.; Evans, T. A.; Seddon, K. R.; Palinko, I. *New J. Chem.* **1999**, 145−152.

imidazolium cation are involved in chlorine atom interactions. Three chlorine atoms are found in close proximity to the C(4)−H bond, two chlorine atoms to the C(2)−H bond, and one chlorine atom to the C(5)−H bond. In addition, a chlorine atom closely approaches one face of the aromatic ring at a distance of 3.18 Å from the mean 5-atom plane. The dimensions of all of the C−H···Cl interactions are tabulated in Table 5. Predictably, the shorter Cl···H distances correlate with the larger C−H···Cl angles. Those shorter than 3.0 Å have angles of from 145 to 160°. Those longer than 3.0 Å have angles of from 123 to 132°. The ranges of distances and angles in Table 5 are representative of the cation/anion interactions in all of the structures containing hexachlorinated carborane anions (see Experimental Section). For the hexabromocarborane structure **3** the shortest C−H···Br distance is 2.79 Å and the C−H···Br angle is 167°. All of the hexachlorocarborane structures except **8** have a significant Cl atom interaction with the 5-atom π system of the imidazolium ring. Distances to the plane lie in the range 3.13−3.33 Å.

For the compounds that do not contain hexahalogenated carborane anions we do not find any indications of unusually close cations/anion contacts. Given the uncertainty of defining H atom positions we can only say that there are many weak C−H···H−B interactions at about van der Waals H···H separation (2.6 Å).

Conclusion

The inescapable conclusion of this work is that packing inefficiency is the single most important factor in rationalizing the low melting points of *N*,*N*′-dialkylimidazolium salts. Positional disorder of the cations in their crystal structures, a direct indicator of packing inefficiency, has been identified as a common and potentially general characteristic of low melting imidazolium melts with large anions. It is apparent that once cation/anion interactions are reduced essentially to the level of van der Waals or very weak H-bonding-type forces, packing inefficiency becomes reflected in disorder. Packing inefficiency seems to be *the* factor giving *N*,*N*′-dialkylimidazolium salts their low melting points.

The systematic variation of alkyl substituent on the cation *and* the anion has led to usefully predictive trends in melting points. Future work will be directed at optimizing the purity and handling properties of those salts that are liquids at room temperature. By introducing carborane anions into the ionic liquid repertoire, we anticipate that new extremes of cation reactivity can be explored. We are particularly intrigued by the possibility of developing a novel superacid medium that is more strictly non-oxidizing than previously attainable and where the conjugate base (i.e. the anion) has the lowest nucleophilicity presently available.[15]

Acknowledgment. We thank Professor K. R. Seddon (The Queen's University of Belfast) for helpful discussions. This work was supported by the National Science Foundation.

Supporting Information Available: Infrared spectra, elemental analyses, and full crystallographic details: atomic coordinates, anisotropic displacement coefficients, H atom coordinates, packing diagrams, and atom numbering schemes (PDF). This material is available free of charge via the Internet at http://pubs.acs.org.

JA0007511